Angular Dependence of Critical Current and Grain Alignment in Bi-2223 Superconducting Joint

Yasuaki Takeda, Gen Nishijima, Ukyo Nakai, Takanori Motoki, Jun-ichi Shimoyama, and Hitoshi Kitaguchi

***Abstract*—We clarify the relationship between the angular dependence of critical current in a Bi-2223 superconducting joint and the grain alignment of an intermediate layer in the joint. The angular dependence of critical current for the superconducting joint is discussed using a model to describe that for a Bi-2223 tape. Considering an angle of the *c*-axis grain misalignment, the angular dependence is calculated. The misalignment angle is validated from the microstructure observations of the intermediate layer. We can conclude that the *c*-axis grain alignment in the intermediate layer dominates the angular dependence of critical current in the superconducting joint.**

***Index Terms*—Bi-2223 tape, critical current, HTS magnets, microscopy.**

I. Introduction

SUPERCONDUCTING joints are essential if a superconducting magnet is to be operated in persistent mode [1], [2]. Recently, development of superconducting joints between high-temperature superconductors (HTSs) has been significantly progressed [3], [4], [5], [6], [7], [8], [9], [10], [11]. We have developed superconducting joints between multifilamentary $(Bi,Pb)_2Sr_2Ca_2Cu_3O_y$ (Bi-2223) tapes [7], [10], [12]. An intermediate layer of a polycrystalline Bi-2223 thick film is used to form a superconducting joint showing high critical current (I_c).

HTS materials show anisotropic electromagnetic properties. One of the properties is observed in I_c of an HTS tape in a magnetic field with various directions, that is, the angular dependence of I_c. It is important to evaluate the angular dependence of critical current of a superconducting joint (I_{cj}), as in the case of an HTS tape. This is because in a persistent-mode magnet, a magnetic field with various directions may be applied to superconducting joints, depending on the magnet design. Evaluation of the angular dependence of I_{cj} for an HTS joint contributes to not only persistent-mode magnet technology but also materials science of the HTS joints.

In a previous study, we evaluated the angular dependence of I_{cj} for a Bi-2223 closed-loop sample with a superconducting joint [13]. To evaluate in-field I_{cj}, the decay of a current flowing in the closed loop (I_{loop}) was measured, while the superconducting joint of the sample was placed in a magnetic field. The direction of the magnetic field was changed by rotating the sample to obtain the angular dependence of I_{cj}. The evaluation of I_{cj} from current decay measurements provides only I_{cj} lower than the initial I_{loop}. The I_{loop} is introduced into the sample via magnetic induction using a copper coil located at the center of the loop. The initial I_{loop} is limited by the current of the copper coil. This is because the temperature of the copper coil, which is increased due to Joule heating, must be kept sufficiently low. At present, the maximum of the initial I_{loop} is 220 A. In other words, I_{cj} that can be evaluated using this method is up to 220 A so far.

In this study, we discuss the angular dependence of I_{cj} in the Bi-2223 superconducting joint. We use a model that describes the angular dependence of I_c in a Bi-2223 tape considering an angle of the *c*-axis grain misalignment in superconducting filaments [14], [15], [16], [17]. The relationship between the angular dependence of I_{cj} and the grain alignment of an intermediate layer in the superconducting joint is clarified using microstructure observations.

II. Experimental

A Bi-2223 closed-loop sample with a praying-hands-type superconducting joint, which is schematically shown in Fig. 1 and explained in detail in [10], was prepared. The self-inductance (L) of the sample was 1.4 μH. The sample was made from a commercially available Bi-2223 tape with the Ni-alloy mechanical reinforcement (DI-BSCCO Type HT-NX, 4.5 mm wide and 0.25 mm thick [18]). The I_c of the tape is about 180 A at 77 K in self-field and higher than 1 kA at 4 K and 1 T parallel to the tape surface [19]. Both ends of the tape were connected using our joining processes [7], [10], [12], [20]. The reinforcement at both ends was removed. To fabricate a superconducting joint, most of the Bi-2223 filaments were exposed by low-angle polishing at less than 0.5°. The exposed filaments were connected via an intermediate layer, which was equivalent to an about 0.1 mm thick polycrystalline Bi-2223 film. This thick film was synthesized through the slurry process,

Manuscript received 6 October 2023; revised 12 November 2023; accepted 28 November 2023. Date of publication 4 December 2023; date of current version 14 December 2023. This work was supported in part by JST-Mirai Program under Grant JPMJMI17A2, and in part by JSPS KAKENHI under Grant JP22K14482, Japan *(Corresponding author: Yasuaki Takeda.)*

Yasuaki Takeda, Gen Nishijima, and Hitoshi Kitaguchi are with the National Institute for Materials Science (NIMS), Tsukuba, Ibaraki 305-0003, Japan (e-mail: takeda.yasuaki@nims.go.jp).

Ukyo Nakai, Takanori Motoki, and Jun-ichi Shimoyama are with the Aoyama Gakuin University, Sagamihara, Kanagawa 230-0045, Japan (e-mail: shimo@phys.aoyama.ac.jp).

Color versions of one or more figures in this article are available at https://doi.org/10.1109/TASC.2023.3338587.

Digital Object Identifier 10.1109/TASC.2023.3338587

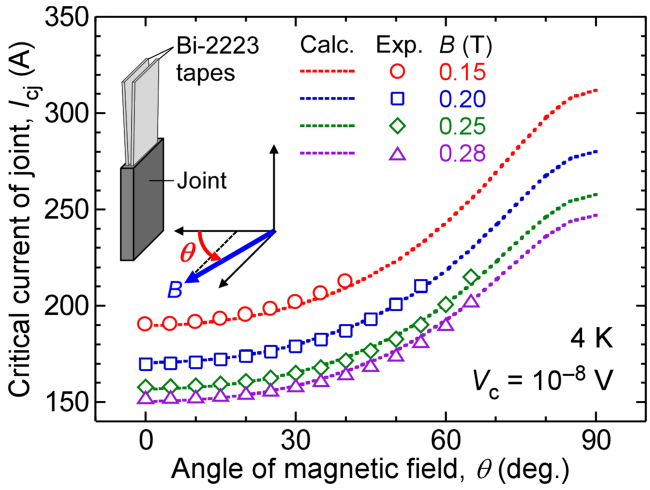

Fig. 1. Angular dependence of calculated and experimentally obtained I_{cj} at 4 K and 0.15–0.28 T. Experimentally obtained values are reported in [13]. Dashed curves, which are calculated using (1) and (5) with $\sigma = 18.6°$, $\alpha = 91.7$ and $\gamma = 0.627$, agree well with experimentally obtained values.

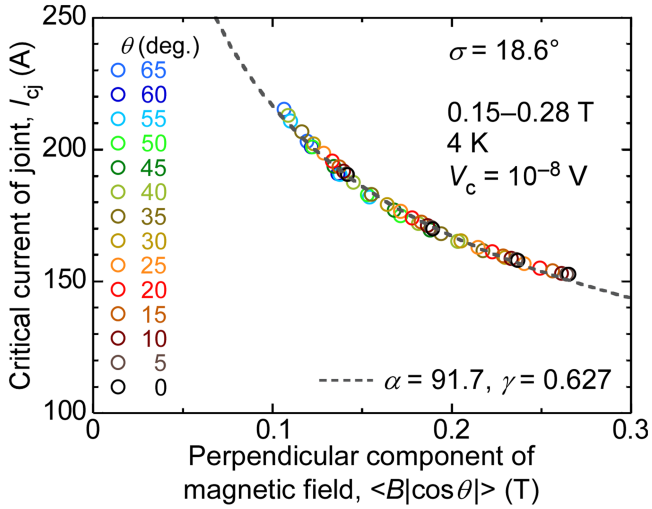

Fig. 2. I_{cj} as a function of perpendicular component of magnetic field calculated using (1) with $\sigma = 18.6°$. Experimentally obtained I_{cj} values appear to be scaled. I_{cj} is fitted using (5) with $\alpha = 91.7$ and $\gamma = 0.627$ shown in gray dashed curve. This curve agrees well with most of experimentally obtained values.

uniaxial pressing at room temperature, and heat treatments. The intermediate layer is formed almost parallel to the surface of the tapes at the joint.

I_{cj} of the sample at 4 K and 0.15–0.28 T was evaluated from the current decay measurements. Voltage (V) was calculated from time (t) dependence of I_{loop} using the equation of $V = -L(\Delta I_{loop}/\Delta t)$. I_{cj} was determined by I_{loop} at a voltage criterion (V_c) of 10^{-8} V in the obtained V–I_{loop} curve. By applying a horizontal magnetic field to the joint and rotating the sample incrementally around the vertical axis, we evaluated the angular dependence of I_{cj}. Details of the sample fabrication and I_{cj} evaluation, which includes the reason why we chose the magnetic fields of 0.15–0.28 T, are described in [13].

We observed the microstructures of the intermediate layer in the superconducting joint of the sample. The polished surfaces of the transverse cross-sections of the joint were observed. We used a field emission scanning electron microscope (FE-SEM, Hitachi SU-70) to obtain secondary electron images.

III. Results and Discussion

A. Angular Dependence of Critical Current in Bi-2223 Superconducting Joint

The experimentally obtained angular dependence of I_{cj} at 4 K and 0.15–0.28 T is shown in Fig. 1 [13]. The angle of the magnetic field (θ) is determined as schematically shown in Fig. 1. θ of 90° corresponds to a magnetic field parallel to the surface of the tapes at the joint. The experimentally obtained I_{cj} values increase with increasing the angle. This is similar to the angular dependence of I_c in a Bi-2223 tape [16], [17]. As described in Section I, I_{cj} values higher than 220 A at high angles were not evaluated experimentally.

The angular dependence of I_{cj} including at high angles was calculated using a model that describes the angular dependence of I_c in a Bi-2223 tape. This model takes the perpendicular component of a magnetic field (B) applied to a tape into account as follows [15], [17]:

$$\langle B\,|\cos\theta|\rangle = B\int_{-90°}^{90°} G\,(\varphi)\,|\cos\,(\theta+\varphi)|\,\mathrm{d}\varphi, \tag{1}$$

where $G(\varphi)$ is a Gaussian distribution of an angle of the c-axis grain misalignment (φ) in superconducting filaments and given by

$$G\ (\varphi) = \frac{1}{\sigma\sqrt{2\pi}}\ \exp\left(-\frac{\varphi^2}{2\sigma^2}\right). \tag{2}$$

The standard deviation (σ) is reported to be 6–12° for filaments of commercially available Bi-2223 tapes [16], [17], [21]. To determine σ, the scaling function of

$$f\ (\theta) = \langle B\,|\cos\theta|\rangle\ /\ \langle B\,|\cos\,(0)|\rangle \tag{3}$$

can be used. The relationship between σ and $f\,(90°)$ of

$$\sigma\ [°] =\ 70.9 f\,(90°) \tag{4}$$

is valid with 1% accuracy in σ ranging from 0 to 20° [15]. By comparing the measurement results at $\theta = 0$ and 90°, σ can be determined.

From current decay measurements at $\theta = 90°$, we experimentally obtained the I_{cj} values of 155 and 173 A at 0.70 and 1.0 T, respectively. From the comparison of these I_{cj} values with the I_{cj} values at 0.15–0.28 T and $\theta = 0$, we obtained $\sigma = 18.6°$ using (4). This σ is larger than the reported values for filaments of commercially available tapes (6–12°) [16], [17], [21]. Given that I_{cj} is mainly dominated by I_c of an intermediate layer [22], the larger σ probably corresponds to the grain misalignment of the Bi-2223 intermediate layer in the superconducting joint.

Fig. 2 shows I_{cj} as a function of the perpendicular component of the magnetic field calculated using (1) and $\sigma = 18.6°$. The experimentally obtained I_{cj} values at 0.15–0.28 T and 0–65° appear to be scaled by <$B|\cos\theta|$>, as demonstrated in Bi-2223 tapes [15], [16], [17]. This suggests that the model for a tape is applicable to the superconducting joint.

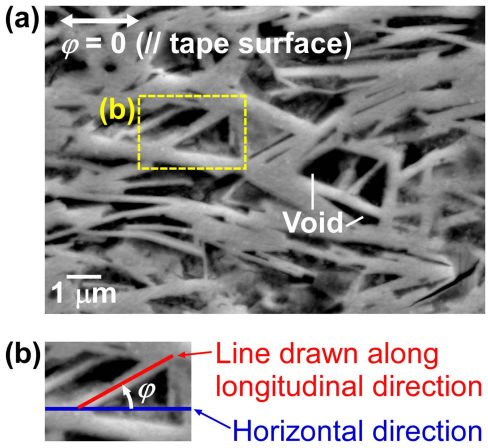

Fig. 3. (a) Secondary electron image of polished surface of transverse cross-section of intermediate layer of superconducting joint. Grains appeared to be weakly aligned. (b) Magnified view of a grain to indicate how to measure φ of the grain.

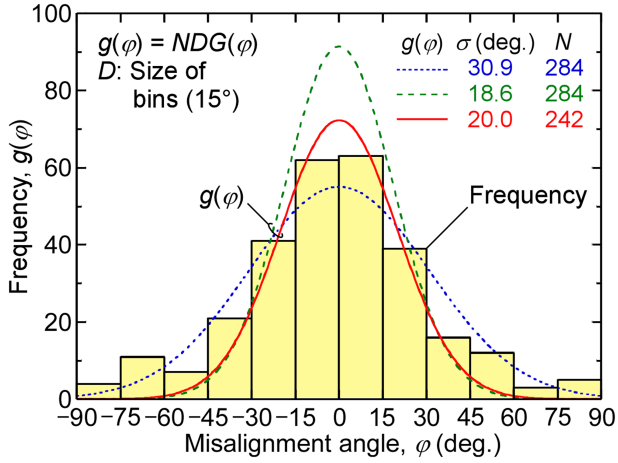

Fig. 4. Histogram of misalignment angle φ. Three $g(\varphi)$ curves are also displayed. Red solid curve is good agreement with histogram at $|\varphi| \leq 45°$. This suggests that at $|\varphi| \leq 45°$, φ distribution approximately follows Gaussian distribution with $\sigma = 20.0°$.

I_{cj} shown in Fig. 2 was fitted to the Irie-Yamafuji model, that is,

$$I_{cj} = \alpha(\langle B\,|\cos\theta|\rangle)^{\gamma-1}, \tag{5}$$

where α and γ are the fitting parameters estimated from the experimental results [23]. We obtained $\alpha = 91.7$ and $\gamma = 0.627$ from the fitting using the least squares method, as shown in the gray dashed curve of Fig. 2. This fitting curve, which agrees well with most of the experimentally obtained values, underestimates the highest I_{cj} value by 1.79%. An equation considering scaling laws for the pinning force density may better describe I_{cj} [17]. This equation could not be used in this study owing to the insufficient data on I_{cj} to apply the scaling laws.

The calculated angular dependence of I_{cj} at 0.15–0.28 T is shown in dashed curves of Fig. 1. For the calculation, we used (1) and (5) with $\sigma = 18.6°$, $\alpha = 91.7$, and $\gamma = 0.627$. The calculated I_{cj} agrees well with the experimentally obtained values at low angles. We estimated I_{cj} values at high angles, which were not experimentally evaluated in the previous study [13]. Considering that the model describes well the angular dependence of I_c in tapes and reproduces the I_{cj} values at low angles, we believe that the angular dependence of I_{cj} is appropriately described including at high angles.

B. Grain Misalignment of Intermediate Layer Evaluated From Microstructural Observations

The large σ value obtained in the previous section probably corresponds to the *c*-axis grain misalignment in the intermediate layer. To evaluate σ directly, the distribution of the *c*-axis grain misalignment angle (φ) was examined from the microstructural observations of the intermediate layer. Fig. 3(a) shows a secondary electron image of the polished surface of the transverse cross-section of the intermediate layer. The horizontal direction is parallel to the tape surface at the joint, corresponding to $\varphi = 0$. Typical plate-like Bi-2223 grains and voids were observed. Many grains showed small φ. As reported in [22], the grains appeared to be weakly *c*-axis-aligned.

We measured φ for each Bi-2223 plate-like grain in three secondary electron images including Fig. 3(a). The size of each image was 13 μm × 8.9 μm. We measured φ for a grain as shown in Fig. 3(b). We drew the straight line along the longitudinal direction of the grain, which is orthogonal to the direction of the *c*-axis. φ corresponded to the counterclockwise angle formed by the line and horizontal direction. The φ values of all grains in the three images were measured. In the case of Fig. 3(a), φ values of 84 grains were measured. The total number of the grains which we measured φ was 284.

Fig. 4 shows a histogram of the misalignment angle φ. The average of φ ($\bar{\varphi}$) and standard deviation (σ) were $-1.2°$ and 30.9°, respectively. The histogram shows quantitatively that the grains are weakly aligned, which agrees with the qualitative impression obtained from Fig. 3(a).

The model to calculate the angular dependence of I_{cj} assumes a Gaussian distribution of φ. We compared the histogram to the Gaussian distribution described using (2). $\bar{\varphi}$ was too small and neglected. Considering $\int_{-90°}^{90°} G(\varphi)\mathrm{d}\varphi \cong 1$, we used $g(\varphi) = NDG(\varphi)$, where N and D were the sum of the frequencies and the size of bins (15°), respectively. $\int_{-90°}^{90°} g(\varphi)\mathrm{d}\varphi$ nearly corresponds to the sum of the area of the bins in the histogram, ND.

Three $g(\varphi)$ curves are displayed in Fig. 4. The blue dotted curve is $g(\varphi)$ with $\sigma = 30.9°$ and $N = 284$. This σ was obtained from the distribution over the entire φ. The green dashed curve is $g(\varphi)$ with $\sigma = 18.6°$ and $N = 284$. This σ corresponds to that used in the previous section. However, these two $g(\varphi)$ curves appeared to disagree with the histogram.

Hensel et al. proposed the railway-switch model, suggesting that the small-angle *c*-axis tilt grain boundaries were the current path in filaments of a Bi-2223 tape [24], [25]. Applying this model, the grains with large $|\varphi|$ will not contribute to I_{cj}. Assuming that the bins of $|\varphi| \geq 45°$ can be neglected, $\bar{\varphi} = -0.4°$, $\sigma = 20.0°$, and $N = 242$ are obtained. Corresponding $g(\varphi)$ is shown by the red solid curve in Fig. 4. The $\bar{\varphi}$ was too small and neglected. This solid curve is in better agreement with the

histogram at $|\varphi| \leq 45°$ than the dashed and dotted curves. This implies that at $|\varphi| \leq 45°$, the distribution of the misalignment angle φ approximately follows the Gaussian distribution described using (2) and $\sigma = 20.0°$.

C. Discussion

In Section III-A, we used the standard deviation σ of 18.6° to calculate the angular dependence of I_{cj}. This σ was larger than those reported for tapes. In Section III-B, the microstructural observations suggested that the distribution of the c-axis grain misalignment angle φ in the intermediate layer follows the Gaussian distribution described using (2) and $\sigma = 20.0°$ at $|\varphi| \leq 45°$. This σ is close to the large value of 18.6°. The large σ used in calculating the angular dependence of I_{cj} is validated from the microstructural observations.

The model that describes the angular dependence of I_c of a tape [14], [15], [16], [17] assumes a Gaussian distribution of the misalignment angle. As explained in Section III-A, this model can also describe the angular dependence of I_{cj} using the large σ of 18.6°. The microstructural observations of the intermediate layer validated this large σ and the Gaussian distribution of the misalignment angle. We can conclude that the c-axis grain alignment in the intermediate layer dominates the angular dependence of I_{cj}.

In the microstructural observations of the intermediate layer, 15% of the total grains showed $|\varphi| \geq 45°$. Because the grains with $|\varphi| \geq 45°$ will not contribute to the current path, the reduction of these grains by improving the grain alignment will be effective to increase I_{cj}. In addition, a decrease in σ increases I_c of a tape [21]. This also suggests that the improvement of the grain alignment in the intermediate layer to decrease σ is promising for increasing I_{cj}.

The c-axis grain alignment of a thick film can be improved by mechanical processes using a uniaxial pressure [26]. Uniaxial pressing at a high pressure will be effective to improve the alignment of an intermediate layer. In this case, mechanical damage of superconducting filaments of joined tapes must be suppressed, as shown in our previous study [22]. An alignment technique using a magnetic field is also effective for the improvement [27], [28].

If the grain alignment of an intermediate layer is improved, higher I_{cj} will be achieved. In contrast, this improvement of the grain alignment will also result in the stronger angular dependence of I_{cj} owing to smaller σ. Fig. 5 shows the calculated angular dependence of I_{cj} at 4 K and 0.15 T. The I_{cj} value is normalized by that at $\theta = 0$. For the calculation, we used (1) and (5) with σ of 6.0–30.0°, $\alpha = 91.7$, and $\gamma = 0.627$. The black solid curve with $\sigma = 18.6°$ corresponds to the calculated angular dependence of I_{cj} shown in Fig. 1. Inset shows normalized I_{cj} at 90° as a function of σ. At low angles, normalized I_{cj} is independent on σ. However, normalized I_{cj} at high angles is strongly dependent on σ. When σ decreases from 18.6° to 6.0° (σ for a tape reported in [21]), normalized I_{cj} at 90° increases from 1.64 to 2.51. This calculation shows that improvement of the grain alignment results in the stronger angular dependence of I_{cj}.

The stronger angular dependence may not be suitable for applying superconducting joints to a persistent-mode magnet.

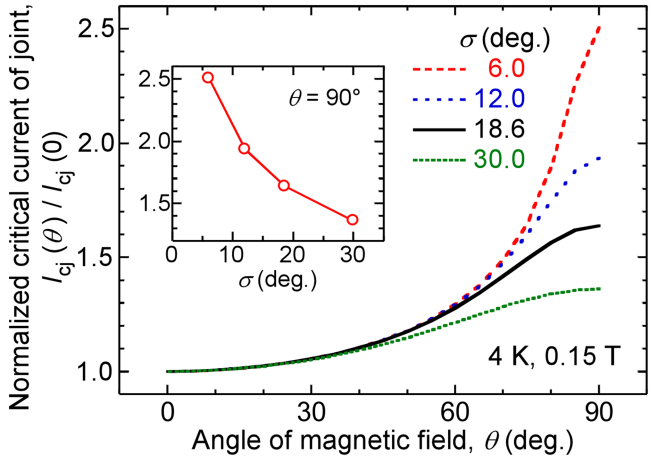

Fig. 5. Calculated angular dependence of I_{cj} at 4 K and 0.15 T. I_{cj} values are normalized by that at $\theta = 0$. Inset shows normalized I_{cj} at 90° as a function of σ. Improvement of grain alignment results in stronger angular dependence.

This is because a magnetic field with various directions may be applied to the joints, depending on the magnet design. The angular dependence of I_{cj} should be discussed not only in materials science, as in this study, but also in persistent-mode magnet technology.

IV. Conclusion

The relationship between the angular dependence of I_{cj} in the Bi-2223 superconducting joint and the grain alignment of the intermediate layer was clarified. The angular dependence of I_{cj} was calculated using the model for a Bi-2223 tape, considering the angle of the c-axis grain misalignment. The calculated I_{cj} agreed well with the experimental results. We estimated I_{cj} that was not evaluated experimentally. The microstructural observations suggested that the distribution of the misalignment angle in the intermediate layer approximately followed the Gaussian distribution. The standard deviation of the misalignment angle used in calculating the angular dependence was validated. We concluded that the c-axis grain alignment in the intermediate layer dominated the angular dependence of I_{cj}.

The improvement of the grain alignment will result in higher I_{cj} and the stronger angular dependence. The angular dependence should be discussed not only in materials science, as in this study, but also in persistent-mode magnet technology.

References

[1] G. D. Brittles, T. Mousavi, C. R. M. Grovenor, C. Aksoy, and S. C. Speller, "Persistent current joints between technological superconductors," *Supercond. Sci. Technol.*, vol. 28, no. 9, Aug. 2015, Art. no. 093001.

[2] Y. Takeda, H. Maeda, K. Ohki, and Y. Yanagisawa, "Review of the temporal stability of the magnetic field for ultra-high field superconducting magnets with a particular focus on superconducting joints between HTS conductors," *Supercond. Sci. Technol.*, vol. 35, no. 4, Apr. 2022, Art. no. 043002.

[3] Y. Park, M. Lee, H. Ann, Y. H. Choi, and H. Lee, "A superconducting joint for $GdBa_2Cu_3O_{7-\delta}$-coated conductors," *NPG Asia Mater*, vol. 6, May 2014, Art. no. e98.

[4] K. Ohki et al., "Fabrication, microstructure and persistent current measurement of an intermediate grown superconducting (iGS) joint between REBCO-coated conductors," *Supercond. Sci. Technol.*, vol. 30, no. 11, Oct. 2017, Art. no. 115017.

[5] P. Chen et al., "Development of a persistent superconducting joint between Bi-2212/Ag-alloy multifilamentary round wires," *Supercond. Sci. Technol.*, vol. 30, no. 2, 2017, Art. no. 025020.
[6] S. Mukoyama et al., "Superconducting joint of REBCO wires for MRI magnet," *J. Phys.: Conf. Ser.*, vol. 1054, 2018, Art. no. 012038.
[7] Y. Takeda et al., "High I_c superconducting joint between Bi2223 tapes," *Appl. Phys. Exp.*, vol. 12, no. 2, Feb. 2019, Art. no. 023003.
[8] X. Jin et al., "Superconducting joint between multi-filamentary $Bi_2Sr_2Ca_2Cu_3O_{10+\delta}$ tapes based on incongruent melting for NMR and MRI applications," *Supercond. Sci. Technol.*, vol. 32, no. 3, Feb. 2019, Art. no. 035011.
[9] T. Mousavi, S. Santra, Z. Melhem, S. Speller, and C. Grovenor, "Superconducting joint structures for Bi-2212 wires using a powder-in-tube technique," *IEEE Trans. Appl. Supercond.*, vol. 31, no. 5, Aug. 2021, Art. no. 6400504.
[10] Y. Takeda et al., "Critical current improvement and resistance evaluation of superconducting joint between Bi2223 tapes," *Supercond. Sci. Technol.*, vol. 35, no. 2, Feb. 2022, Art. no. 02LT02.
[11] D. Huang et al., "An efficient approach for superconducting joint of YBCO coated conductors," *Supercond. Sci. Technol.*, vol. 35, no. 7, May 2022, Art. no. 075004.
[12] Y. Takeda, G. Nishijima, K. Kobayashi, and H. Kitaguchi, "Fabrication of Bi-2223 superconducting joint by hot-pressing process," *IEEE Trans. Appl. Supercond.*, vol. 33, no. 5, Aug. 2023, Art. no. 6400207.
[13] Y. Takeda, G. Nishijima, U. Nakai, T. Motoki, J. Shimoyama, and H. Kitaguchi, "Angular dependence of resistance and critical current of a Bi-2223 superconducting joint," *Supercond. Sci. Technol.*, vol. 36, no. 12, Oct. 2023, Art. no. 125010.
[14] L. N. Bulaevskii, L. L. Daemen, M. P. Maley, and J. Y. Coulter, "Limits to the critical current in high-T_c superconducting tapes," *Phys. Rev. B*, vol. 48, no. 18, pp. 13798–13816, Nov. 1993.
[15] O. van der Meer, B. ten Haken, and H. H. J. ten Kate, "A model to describe the angular dependence of the critical current in a Bi-2223/Ag superconducting tape," *Physica C*, vol. 357–360, no. 2, pp. 1174–1177, Aug. 2001.
[16] P. Sunwong, J. S. Higgins, and D. P. Hampshire, "Angular, temperature, and strain dependencies of the critical current of DI-BSCCO tapes in high magnetic fields," *IEEE Trans. Appl. Supercond.*, vol. 21, no. 3, pp. 2840–2844, Jun. 2011.
[17] D. Kobayashi, T. Okada, and S. Awaji, "High-field critical current properties of $(Bi, Pb)_2Sr_2Ca_2Cu_3O_y$ filaments," *IEEE Trans. Appl. Supercond.*, vol. 32, no. 4, Jun. 2022, Art. no. 6400105.
[18] T. Nakashima et al., "Drastic improvement in mechanical properties of DI-BSCCO wire with novel lamination material," *IEEE Trans. Appl. Supercond.*, vol. 25, no. 3, Jun. 2015, Art. no. 6400705.
[19] M. Bonura, C. Barth, and C. Senatore, "Electrical and thermo-physical properties of Ni-alloy reinforced Bi-2223 conductors," *IEEE Trans. Appl. Supercond.*, vol. 29, no. 5, Aug. 2019, Art. no. 6400205.
[20] Y. Takeda et al., "Development of a persistent current mode 9.39 T (400 MHz) LTS/Bi-2223 NMR magnet with a Bi-2223 superconducting joint," *IEEE Trans. Appl. Supercond.*, vol. 32, no. 6, Sep. 2022, Art. no. 4301005.
[21] K. Sato, S. Kobayashi, and T. Nakashima, "Present status and future perspective of bismuth-based high-temperature superconducting wires realizing application systems," *Jpn. J. Appl. Phys.*, vol. 51, Dec. 2012, Art. no. 010006.
[22] Y. Takeda, G. Nishijima, K. Inoue, Y. Takano, and H. Kitaguchi, "The effect of intermediate layer densification on the critical current of a Bi-2223 superconducting joint," *Supercond. Sci. Technol.*, vol. 36, no. 3, Jun. 2023, Art. no. 035004.
[23] F. Irie and K. Yamafuji, "Theory of flux motion in non-ideal type-II superconductors," *J. Phys. Soc. Jpn.*, vol. 23, no. 2, pp. 255–268, Aug. 1976.
[24] B. Hensel, J.-C. Grivel, A. Jeremie, A. Perin, A. Pollini, and R. Flükiger, "A model for the critical current in $(Bi,Pb)_2Sr_2Ca_2Cu_3O_x$ silver-sheathed tapes: The role of small-angle c-axis grain boundaries and of the texture," *Physica C*, vol. 205, no. 3–4, pp. 329–337, Feb. 1993.
[25] B. Hensel, G. Grasso, and R. Flükiger, "Limits to the critical transport current in superconducting $(Bi,Pb)_2Sr_2Ca_2Cu_3O_{10}$ silver-sheathed tapes: The railway-switch model," *Phys. Rev. B*, vol. 51, no. 21, pp. 15456–15473, Jun. 1995.
[26] T. Asano, Y. Tanaka, M. Fukutomi, K. Jikihara, J. Machida, and H. Maeda, "Preparation of highly oriented microstructure in the (Bi,Pb)-Sr-Ca-Cu-O sintered oxide superconductor," *Jpn. J. Appl. Phys.*, vol. 27, no. 9, pp. L1652–L1654, Sep. 1988.
[27] S. Horii, R. Nagai, M. Yamaki, T. Maeda, J. Shimoyama, and T. Doi, "Magnetic tri-axial grain alignment achieved in bismuth-based cuprate superconductors," *Appl. Phys. Exp.*, vol. 6, no. 9, Sep. 2013, Art. no. 093102.
[28] Y. Takeda, T. Iwami, Y. Saito, T. Motoki, and J. Shimoyama, "Fabrication of high J_c Bi2223 thick films through grain alignment technique using a permanent magnet," *Physica C: Supercond*, vol. 584, no. 15, May 2021, Art. no. 1353873.